Materials Science Forum vols. 308-311 (1999) pp 971-976
© (1999) Trans Tech Publications, Switzerland
doi:10.4028/www.scientific.net/MSF.308-311.971

Gradient Elasticity Theory for a Mode III Crack in a Functionally Graded Material

G.H. Paulino[1], A.C. Fannjiang[2] and Y.-S. Chan[2]

[1] Department of Civil & Environmental Engineering, and Graduate Group in Applied Mathematics (GGAM) University of California, Davis, CA 95616, USA

[2] Department of Mathematics, University of California, Davis, CA 95616, USA

Keywords: Functionally Graded Materials, Gradient Elasticity, Fracture Mechanics, Mode III Crack, Cohesive Zone Model, Fredholm Integral Equation, Hypersingular Integrals

Abstract. Anisotropic strain gradient elasticity theory is applied to the solution of a mode III crack in a functionally graded material (FGM). The theory includes both volumetric and surface energy terms, and a particular form of the moduli variation. The crack boundary value problem is solved by means of Fourier transform and a hypersingular integral equation of the Fredholm type. The solution naturally leads to a cusping crack, which is consistent with Barenblatt's "cohesive zone" theory, but without the assumption regarding existence of interatomic forces. The numerical implementation is discussed and examples are given, which provide insight into the cracking phenomenon in FGMs governed by strain gradient elasticity with characteristic lengths associated to volumetric and surface strain energy terms.

1 Introduction

Modeling of anti-plane shear cracks in functionally graded materials (FGMs) has been a subject of much interest because this is a relatively simple problem to work with, and it provides relevant information about fracture behavior in non-homogeneous materials [1, 2]. Based on the original work by Casal [3], Vardoulakis *et al.* [4] have recently presented a gradient elasticity theory with volumetric and surface energy terms for mode III cracks in homogeneous materials. To the best of the authors' knowledge, there is no work in the literature regarding modeling of crack problems in FGMs using gradient elasticity. This is the subject of this paper, which addresses mode III cracks (tearing mode). The objective is to present a technique which lead to analytically and computationally tractable solutions of the problem, and to provide examples comparing the results of various types of material microstructure (described by characteristic lengths) and gradation (described by moduli functions).

2 Formulation of the Problem

Consider the antiplane shear crack problem for a semi-infinite nonhomogeneous elastic medium shown in Fig. 1. The displacement components (u_x, u_y, u_z) satisfy the relations

$$u_x = 0, \quad u_y = 0, \quad u_z \equiv w(x, y) \quad . \tag{1}$$

Let the shear modulus G be a function of y only, and assume

$$G = G(y) = G_0 e^{\gamma y} \quad , \tag{2}$$

where G_0 and γ are known constants. In this case, the constitutive equations of gradient elasticity for an FGM are [4]:

$$\begin{aligned}
&\sigma_{xx} = \sigma_{yy} = \sigma_{xy} = \sigma_{zz} = 0 \quad , \\
&\sigma_{xz} = 2G(y)(\epsilon_{xz} - \ell^2 \nabla^2 \epsilon_{xz}) \quad , \quad \sigma_{yz} = 2G(y)(\epsilon_{yz} - \ell^2 \nabla^2 \epsilon_{yz}) \quad , \\
&\mu_{xxz} = 2G(y)\ell^2 \frac{\partial \epsilon_{xz}}{\partial x} \quad , \quad \mu_{xyz} = 2G(y)\ell^2 \frac{\partial \epsilon_{yz}}{\partial x} \quad , \\
&\mu_{yxz} = 2G(y)\left(\ell' \epsilon_{xz} + \ell^2 \frac{\partial \epsilon_{xz}}{\partial y}\right) \quad , \quad \mu_{yyz} = 2G(y)\left(\ell' \epsilon_{yz} + \ell^2 \frac{\partial \epsilon_{yz}}{\partial y}\right) \quad ,
\end{aligned} \tag{3}$$

where ℓ and ℓ' are material lengths associated to volumetric and surface elastic strain energy, respectively; σ_{ij} is the stress tensor; and μ_{ijk} is the couple-stress tensor. Here, the infinitesimal strain tensor is defined in the usual manner as

$$\epsilon_{xz} = \frac{1}{2}\frac{\partial w}{\partial x} \quad , \quad \epsilon_{yz} = \frac{1}{2}\frac{\partial w}{\partial y} \quad , \tag{4}$$

and all other components of the strain tensor vanish.

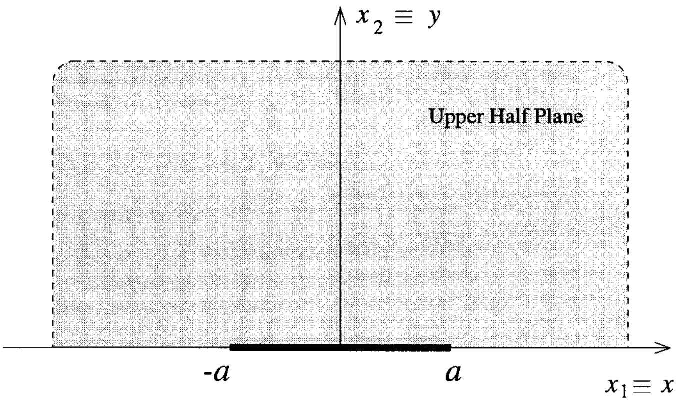

Fig. 1. Geometry for the mode III crack problem.

The following mixed boundary conditions are considered

$$\begin{aligned}
&\sigma_{yz}(x,0) = p(x) \ , |x| < a \\
&\mu_{yyz}(x,0) = 0 \ , \quad -\infty < x < \infty \\
&w(x,0) = 0 \ , \qquad |x| > a
\end{aligned} \tag{5}$$

together with the single-valuedness condition

$$\boxed{\int_{-a}^{a} \phi(x)dx = 0} \ , \tag{6}$$

where

$$\phi(x) = \frac{\partial}{\partial x} w(x, 0^+) \tag{7}$$

and

$$\phi(x) = 0 \ , \quad |x| > a \quad . \tag{8}$$

3 Governing Differential Equations

The only non-trivial equilibrium equation is

$$\frac{\partial \sigma_{xz}}{\partial x} + \frac{\partial \sigma_{yz}}{\partial y} = 0 \quad . \tag{9}$$

Using Eqs. (3) and (4), together with Eq. (9), one obtains the following governing partial differential equation (PDE)

$$\frac{\partial}{\partial x}\left[G(y)\left(\frac{\partial w}{\partial x} - \ell^2\nabla^2\frac{\partial w}{\partial x}\right)\right] + \frac{\partial}{\partial y}\left[G(y)\left(\frac{\partial w}{\partial y} - \ell^2\nabla^2\frac{\partial w}{\partial y}\right)\right] = 0 \quad , \tag{10}$$

which can be rewritten as

$$\boxed{-\ell^2\nabla^4 w - \gamma\ell^2\nabla^2\tfrac{\partial w}{\partial y} + \nabla^2 w + \gamma\tfrac{\partial w}{\partial y} = 0} \quad , \tag{11}$$

or

$$\boxed{(1-\ell^2\nabla^2)(\nabla^2 + \gamma\tfrac{\partial}{\partial y})w = 0} \quad . \tag{12}$$

The PDE (12) is a double perturbation of the classical governing equation for linear elastic fracture mechanics (LEFM). By taking $\gamma \to 0$, one recovers the PDE for gradient elasticity, which is a composition of the harmonic and Helmholtz equations. Furthermore, by taking both $\gamma \to 0$ and $\ell \to 0$, one obtains the well known harmonic equation for mode III, according to LEFM.

By applying Fourier transform method, the PDE (11) can be converted into the following ordinary differential equation (ODE)

$$\boxed{\left[\ell^2\tfrac{d^4}{dy^4} + \gamma\ell^2\tfrac{d^3}{dy^3} - (2\ell^2\xi^2+1)\tfrac{d^2}{dy^2} - \gamma(1+\ell^2\xi^2)\tfrac{d}{dy} + (\ell^2\xi^4+\xi^2)\right]W = 0} \tag{13}$$

where $W(\xi)$ is the Fourier transform of $w(x)$.

4 Hypersingular Integral Equation

Using the framework described above and after a number of intense algebraic steps [5], one arrives at the governing Fredholm integral equation

$$\frac{G}{2}(\ell' - \ell^2\gamma)\phi'(x) + \frac{G}{\pi}\int_{-a}^{a}\left\{\frac{-2\ell^2}{(t-x)^3} + \frac{\frac{\ell^2\gamma^2}{8} - \frac{3\ell'\gamma}{8} + 1 - (\frac{\ell'}{2\ell})^2}{t-x} + k(x,t)\right\}\phi(t)\,dt \;=\; p(x) \quad , |x| < a \tag{14}$$

which contains both the hypersingular and Cauchy singular kernels. The kernel $k(x,t)$ is regular and this kernel together with all the details of the derivations are presented in Reference [5].

5 Numerical Aspects and Derivation of Physical Quantities

In order to solve for the unknown slope function $\phi(t)$ in the hypersingular Fredholm integral equation (14), the following representation of $\phi(t)$ is chosen

$$\phi(t) = (1-t^2)^{\frac{3}{2}} \sum_{n=0}^{\infty} A_n T_n(t) \ , \tag{15}$$

where A_n's are coefficients to be determined numerically and $T_n(t)$'s are the Chebyshev polynomials of first kind. The collocation method is employed here to transform the integral equation (14) into a system of algebraic linear equations [1, 5]. Note that the variables "x" and "t" refer to collocation and integration points, respectively.

The integrand of Eq. (14) can be partitioned into two parts: a singular part and a non-singular part. The singular part is integrated exactly, and the non-singular part is integrated by means of quadrature. The details on how to solve the cubic hypersingularity numerically can be found in Paulino *et al.* [6].

5.1 Crack Displacement Profile, $w(x,0)$

Once the slope function $\phi(t)$ is found numerically by the representation in Eq. (15), the crack displacement function $w(x,0)$ is readily obtained as

$$w(x,0) = \int_{-1}^{x} \phi(t)dt = \int_{-1}^{x} (1-t^2)^{\frac{3}{2}} \sum_{n=0}^{N} A_n T_n(t)dt \ . \tag{16}$$

where N is the total number of integration points.

5.2 Stress Intensity Factor, K_{III}

Define the mode III stress intensity factor (SIF) K_{III} at the crack tip $x=a$ by

$$K_{III}(a) = \lim_{x \to a^+} \sqrt{2\pi(x-a)}\sigma_{yz}(x,0) \quad , \quad (x > a) \quad . \tag{17}$$

The limit is taken from outside of crack surfaces towards the crack tip. Note that the integral equation (14) is the expression for $\sigma_{yz}(x,0)$, which is also valid for $|x| > a$. The key point is to evaluate the hypersingular term from outside the crack surfaces. After some lengthy algebra, the normalized mode III SIF is obtained as in References [5, 6]

$$K_{III}(1) = -3\sqrt{\pi}\ell^2 \sum_{n=0}^{N} A_n T_n(1) = -3\sqrt{\pi}\ell^2 \sum_{n=0}^{N} A_n \quad . \tag{18}$$

6 Examples

The solution given in this study for a non-homogeneous half plane having a shear modulus $G(y), y > 0$, is also valid for the corresponding infinite medium in which $y = 0$ is a plane of symmetry, *i.e.* $G(-y) = G(y), -\infty < y < \infty$. For all the examples presented, $p(x) = -\sigma_0$ and the normalization $\sigma_0/G = 1$ has been employed. Figures 2 and 3 show the crack displacement profiles for FGMs (*i.e.* varying γ) for gradient elastic materials with different values of the characteristic lengths (ℓ, ℓ'). In both graphs, the broken lines stand for the homogeneous material

($\gamma = 0$) case. Note the cusping at the crack tips, which is consistent with Barenblatt's "cohesive zone" theory [7], but without the assumption regarding existence of interatomic forces. Moreover, for these examples, as γ increases the displacement magnitude decreases, which is consistent with similar results by Erdogan and Ozturk [1] using classical elasticity to model mode III cracks in FGMs.

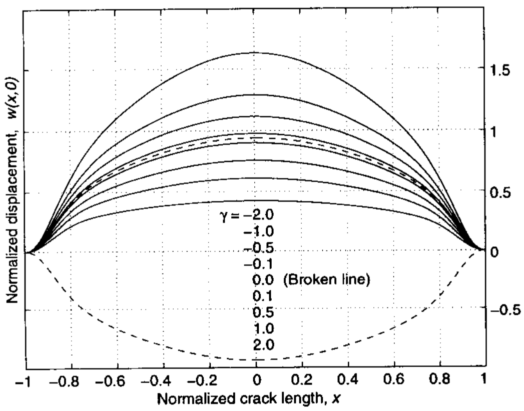

Fig. 2. Crack profiles: $\ell = 0.05$ and $\ell' = 0$.

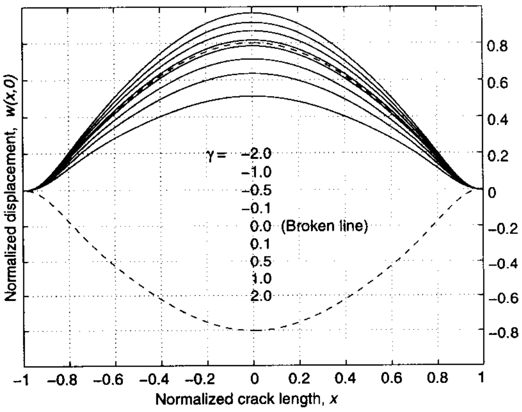

Fig. 3. Crack profiles: $\ell = 0.2$ and $\ell' = 0.1$.

Results for SIFs are reported in Tables 1 and 2. Table 1 shows a comparison for a convergence study involving a non-graded and a graded gradient elastic material with $\ell' = 0$ in both cases. Note that as the number of collocation points (N) increases, the results do converge for both materials. When $\ell' \neq 0$, the SIFs still converge, but the convergence is worse than for the case when $\ell' = 0$. Table 2 lists the SIFs for graded gradient elastic materials considering various values of the material parameter γ and 31 collocation points in the numerical solution. For the function $G(y)$ given by Eq. (2), the SIF monotonically decreases as γ increases. Further numerical results and discussions are provided in Reference [5].

Table 1. Convergence of stress intensity factors. Comparison between a gradient elastic material ($\ell = 0.05$, $\ell' = 0$; $\gamma = 0$) with a graded gradient elastic material ($\ell = 0.05$, $\ell' = 0$; $\gamma = 0.3$). The condition number of the system matrix varies from 10^2 (N=11) to 10^4 (N=61).

N	$\ell = 0.05,\ \ell' = 0;\ \gamma = 0$	$\ell = 0.05,\ \ell' = 0;\ \gamma = 0.3$
11	0.987	0.898
21	0.931	0.844
31	0.925	0.839
41	0.925	0.839
51	0.925	0.839
61	0.925	0.839

7 Concluding Remarks

This paper has presented a theory and corresponding implementation for modeling anti-plane shear cracks in FGMs using strain gradient elasticity, which includes both volumetric and

Table 2. Stress intensity factors for various values of γ considering two different gradient elastic materials ($\ell = 0.05$, $\ell' = 0$; $\ell'/\ell = 0$ and $\ell = 0.05$, $\ell' = 0$; $\ell'/\ell = 1/2$) and considering N=31.

γ	$\ell = 0.05$, $\ell' = 0$	$\ell = 0.2$, $\ell' = 0.1$
-2.0	1.339	5.153
-1.0	1.152	4.907
-0.5	1.046	4.695
-0.1	0.951	4.463
0.0	0.925	4.392
0.1	0.896	4.310
0.5	0.785	3.970
1.0	0.671	3.586
2.0	0.521	3.010

surface energy terms. The characteristic lengths associated to these terms are assumed to be constant, and the shear modulus is assumed to have a particular functional variation, according to Eq. (2). The present hypersingular integral equation approach leads to a numerically tractable solution of the problem, and relevant fracture mechanics results have been reported. These results include crack displacement profiles and stress intensity factors. Potential extension of this work include investigation of fracture mechanics of functionally graded gradient elastic materials in mode I and mixed mode (*i.e.* combined modes I and II).

Acknowledgements

We acknowledge the support from the USA National Science Foundation (NSF) through grants CMS-9713798 (Mechanics & Materials Program) and DMS-9600119.

References

[1] F. Erdogan and M. Ozturk. Diffusion problems in bonded nonhomogeneous materials with an interface cut. *Int. J. Eng. Sci.*, 30(10):1507–1523, 1992.

[2] M. Ozturk and F. Erdogan. Antiplane shear crack problem in bonded materials with a graded interfacial zone. *Int. J. Eng. Sci.*, 31(12):1641–1657, 1993.

[3] P. Casal. La capilarité interne. *Cahier du Groupe Français d'Études de Rhéology C.N.R.S.*, VI(3):31–37, 1961.

[4] I. Vardoulakis, G. Exadaktylos, and E. Aifantis. Gradient elasticity with surface energy: Mode-III crack problem. *Int. J. Solids Struct.*, 33(30):4531–4559, 1996.

[5] G. H. Paulino, A. C. Fannjiang, and Y.-S. Chan. Gradient elasticity theory for mode III cracks in functionally graded materials. *To be submitted for journal publication.*

[6] G. H. Paulino, Y.-S. Chan, and A. C. Fannjiang. Gradient elasticity with volumetric and surface energy applied to mode III cracks, revisited. *To be submitted for journal publication.*

[7] G. I. Barenblatt. The mathematical theory of equilibrium cracks in brittle fracture. *Adv. Appl. Mech.*, 7:55–129, 1962.

This article was processed using the LaTeX macro package with TTP style

Functionally Graded Materials

doi:10.4028/www.scientific.net/MSF.308-311

Gradient Elasticity Theory for a Mode III Crack in a Functionally Graded Material

doi:10.4028/www.scientific.net/MSF.308-311.971